Low consistency refining of mechanical pulp: Relationships between refiner operating conditions and pulp properties

Antti Luukkonen, James A. Olson, and D. Mark Martinez

KEYWORDS: LC Refining, Pulp properties, Fibre properties, Modeling

SUMMARY: Various refining models have been created to characterize the refining action; however few models provide relations between operating conditions and resulting changes in pulp/fiber properties. The objective of the article is to construct predictive models for pulp/fiber property changes from LC refiner operating condition.

Here mechanical pulps are characterized by fiber length and freeness which have been previously shown to correlate with other pulp and handsheet properties.

The predictive models are created from data collected from pilot and mill flat disc LC refiners with different diameters to gain insight for the governing factors for scaling results. The intent is to use the models to maximize pulp quality development during LC refining of mechanical pulp.

ADDRESSES OF THE AUTHORS: Antti Luukkonen (antti.luukkonen@andritz.com) Andritz R&D pilot plant, 3200 Upper Valley Pike, Springfield, OH, USA, **James Olson** (james.olson@ubc.ca), **D. Mark Martinez** (martinez@chbe.ubc.ca) University of British Columbia, Pulp and Paper Center, 2385 East Mall, Vancouver, BC V6T 1Z4, Canada

Corresponding author: Antti Luukkonen

Low consistency (LC) refining of primary high consistency (HC) refined pulp has been shown to be more energy efficient in reaching target freeness in comparison to a two stage HC process (Musselman et al, 1997). Previously published results have shown that a maximum in tensile strength may be achieved in LC treatment when operated at the optimal gap between the rotor and stator plates (Luukkonen et al 2010a) This optimum gap has been showed to be just above the critical gap which is characterized by the onset of significant fibre cutting.

To maximize LC refining efficiency, it is fundamental to understand the relationships between refiner operating conditions and pulp/fiber quality development. Previous refining theories give predictions for the refining intensity and applied energy, but few of them predict resulting pulp quality (Page 1989).

A methodology has been proposed to relate operating conditions to pulp quality (Luukkonen et al 2010b). The methodology first relates refiner operating conditions (power, flow rate, refiner speed and gap) to changes in fibre quality (fibre length and freeness), and secondly fibre quality to pulp handsheet quality (tensile, tear, and bulk). This methodology was developed using a pilot flat disc LC refiner, and therefore the effect of refiner diameter was not completely characterized.

The focus of this work is to gain better understanding in scale-up from pilot LC refining results to the range of different diameter refiners available in industry. The approach taken was to conduct a series of mill trials over a range of refiner diameters, and to develop predictive models relating fibre properties to LC refiner operational variables using dimensional analysis.

The objective is not to propose these predictive models as either universal or definite. The goal is to study the significance of the refining variables tested and further the research for new models to characterize the LC refining action. The design of experiment is not ideal as the tested refiners had different feed mechanical pulp from different species from different geological locations. Yet the results show promising correlations and continue to build upon a new methodology to characterize LC refining.

Materials and Methods

Data for the predictive models was collected from seven refiners: one pilot scale refiner at Andritz R&D facility in Springfield, Ohio, and six different industrial refiners located at various pulp and paper mills in North America and Scandinavia. The conditions tested are presented in the appendix. It should be noted that all of the tested refiners were flat disc refiners with a floating rotor and two refining zones.

The gap size between the rotor and stator was approximated by measuring the linear displacement of the refiner adjustment end using an external LVDT sensor. For a LC refiner with a floating rotor and two separate refining zones the LVDT sensor measured the change in the total gap. The total gap measurement was divided by two to approximate the gap in each refining zone with the assumption that the rotor was perfectly centered. This protocol was used for all refiners tested.

Pilot trials were conducted by refining pulp in a number of passes through the refiner while maintaining constant operating conditions. Details of the experimental protocol have been previously published. Mill LC trials were conducted by running different motor loads for different flow rates, and measuring the pulp quality both before and after refining.The number of variables in the LC refining process elevates the importance of proper scaling between different size refiners. Dimensional analysis is used to reduce the number of independent refining variables by creating nondimensional groups with dimensional scales. Here the dimensional scales for mass, length and time were set as pulp density, ρ [kg/m^3] , here approximated as water for low consistencies of ~4%, refiner diameter D [m], and refiner rotational speed ω [1/s], respectively.

Results

The results are presented in two sections. The first section will continue to study the relationships between refiner operational variables with the addition of fiber length, whereas the second section will study the relationship between applied specific energy and the resulting change in freeness.

Power vs. Gap

It has been previously published that the Net Power Number, $P_{net}/(\rho\omega^3 D^5)$, is somewhat linearly related to the inverse of the dimensionless gap (D/G), and that the mass flow rate of pulp does not affect the net power consumption greatly (Luukkonen et al 2010b). Here G [m] stands for the approximated gap between the rotor and stator refiner plates.

The data in *Fig 1* shows the dimensionless power number plotted with the dimensionless gap. Here, the somewhat linear trend is apparent at lower values of (D/G), but significant scatter is apparent at larger values of this parameter. The increasing scatter is interpreted as other parameters, besides gap and diameter, are important in understanding the net power applied to the suspension.

To help address this, it is considered that the net power is related to both the fibre length (FL) and a parameter related to the plate pattern. In this case we choose the bar edge length (BEL), as defined by TAPPI standard TIP 0508-05 (1994), to characterize the plate design.

Using a dimensional analysis it is assumed that the Net Power Number is related to gap, fibre length and plate design. A statistical analysis of the selected dimensionless groups yields a function of the form:

$$\frac{P_{net}}{\rho\omega^3 D^5} = 0.03\left(\frac{D}{G}\right)^{0.75}\left(\frac{FL}{D}\right)^{1.31}\left(\frac{BEL}{D}\right)^{0.46} \quad [1]$$

To determine the quality of the proposed correlation between the dimensionless groups, the measured Net Power Number values are plotted with values from the proposed model in *Fig 2*. The diagonal line represents a perfect fit between the measured and calculated values. The good correlation seen in *Fig 2* has a R^2=*0.84*.

Regardless of the remaining deviation, the three dimensionless parameters of gap, plate design, and fibre length appear to be sufficient in predicting refiner motor load for the range of conditions tested. The remaining deviation is hypothesized to origin from error in some of the parameters, i.e. BEL, and to the fact that other parameters, for e.g. consistency, were not included in the dimensional analysis. To highlight this, BEL may not accurately characterize the effect of plate pattern, as similar BEL values can be obtained for different combinations of bar and groove widths. However the somewhat linear relationship remains evident with a different slope for each refiner plate design tested. Further, measurement error exists for the estimated gap size, fibre length and no-load power.

Eq 1 indicates that the net power number varies nearly linearly with the inverse of gap size. This finding is slightly different to that reported by Mohlin (2007) who

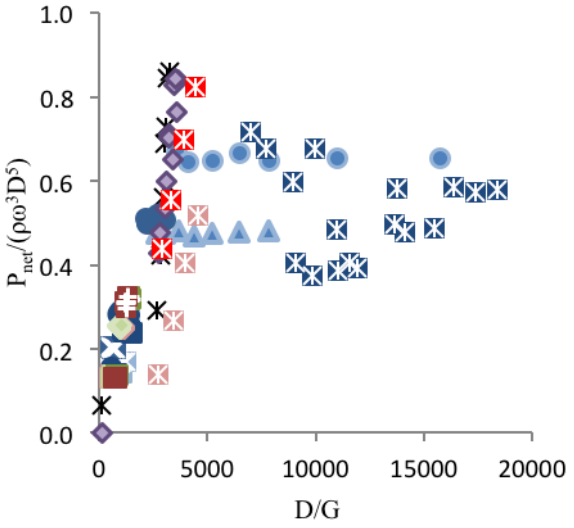

Fig 1. Correlation between Net Power Number and dimensionless gap for both pilot and mill trials.

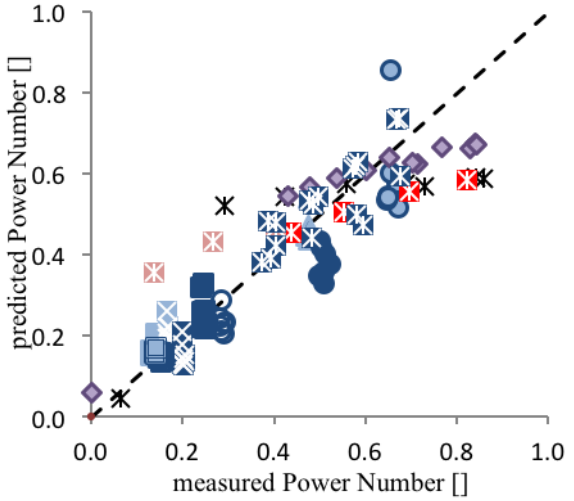

Fig 2. Correlation between predicted and measured Net Power Number for best fit coefficients.

shows that refiner power is inversely proportional to gap size. If we set this relationship to be linear, we find that the following equation describes our data set, see *Eq 2:*

$$\frac{P_{net}}{\rho\omega^3 D^5} = 0.008\left(\frac{D}{G}\right)^{1}\left(\frac{FL}{D}\right)^{\frac{3}{2}}\left(\frac{BEL}{D}\right)^{\frac{1}{2}} \quad [2]$$

The correlation coefficient for this relationship decreases to R^2=*0.73*, see *Fig 3*. but the advantage is the exponents for fibre length and BEL are now fractions. This implies that some underlying physical relationship is governing this behavior. This however has yet to be determined.

Freeness vs. Net Specific Energy

A total of 112 LC refining trial points, from both pilot and mill trials, were measured for Canadian Standard Freeness (CSF) according to TAPPI standard T227. Refiner operating conditions are nondimensionalized similarly as in the power – gap correlation study to reduce the number of independent variables. Net Specific Energy (NSE) is nondimensionalized by both rotational speed and diameter squared.

Fig 4 shows the measured freeness values for increasing dimensionless Net Specific Energy, where similar freeness drop trends exist for both pilot and mill trials and greater freeness drop can be observed for higher feed freeness pulps.

The pilot trials show a notably greater range for dimensionless Net Specific Energy than the mill trials because of the different trial protocol. For the pilot trials Net Specific Energy was increased by running multiple passes through the refiner, whereas mill refining energy is increased by increasing motor load for a constant flow rate.

Based on the trends seen in *Fig 4*, an exponential form is hypothesized for freeness drop as a function of dimensionless Net Specific Energy, where k is considered as a freeness drop coefficient for LC refining of mechanical pulp:

$$CSF_{out} = CSF_{in} \cdot e^{-k\frac{NSE}{\omega^2 D^2}} \quad [3]$$

Values for the freeness drop coefficient k can be solved from *Eq 3*:

$$k = -ln\left(\frac{CSF_{out}}{CSF_{in}}\right) \Big/ \frac{NSE}{\omega^2 D^2} \quad [4]$$

Values for k are calculated from the freeness data in *Fig 4*. Here the pilot trial data with multiple passes through the refiner will be treated as single passes, collecting a k value for each pass.

The refining action is characterized by refining intensity and energy applied. Instead of plate design, gap size is used as the intensity parameter. Therefore the freeness drop coefficient k is proposed to be an exponential multiple regression function of feed freeness and gap size. Feed freeness is selected as different freeness drop rates can be observed in *Fig 4* for different feed freeness pulps.

From a least square fit to the presented data, the following exponential coefficients are obtained:

$$k = \left(\frac{CSF_{in}}{D^3}\right)^{-0.82} \cdot \left(\frac{D}{G}\right)^{-1.41} \quad [5]$$

Substituting k from *Eq 5* back into the freeness drop model in *Eq 3* gives the following formula for discharge freeness as a function of feed freeness, gap size, and applied dimensionless Net Specific Energy:

$$CSF_{out} = CSF_{in} \cdot exp\left(-\left(\frac{D^3}{CSF_{in}}\right)^{0.82} \left(\frac{G}{D}\right)^{1.41} \frac{NSE}{\omega^2 D^2}\right) \quad [6]$$

The R^2=*0.98* for the data points shown in *Fig 5* indicate good model accuracy for the range of conditions tested.

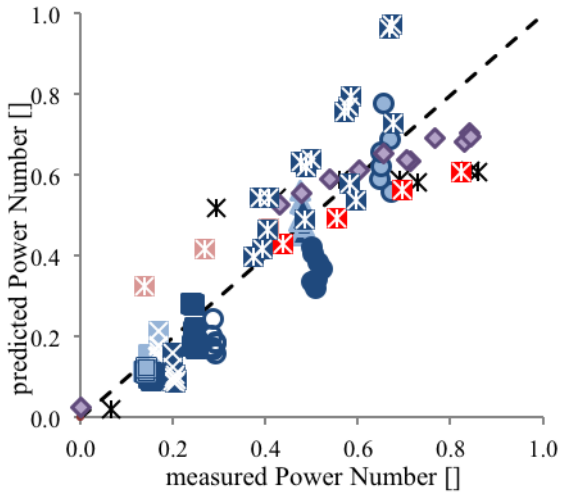

Fig 3. Correlation between the predicted and measured Power Number for approximated coefficients.

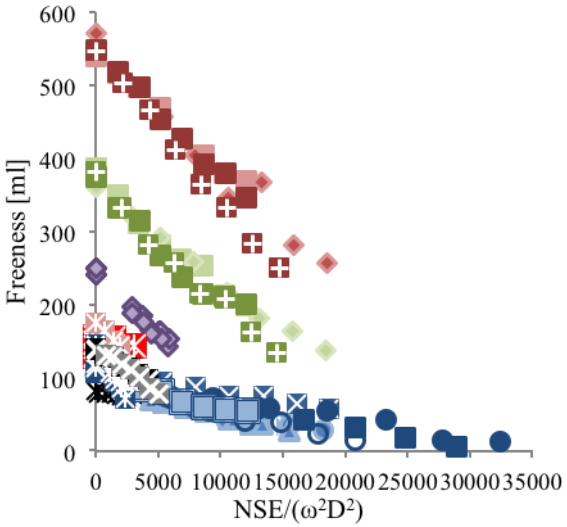

Fig 4. Freeness drop for increasing dimensionless Net Specific Energy.

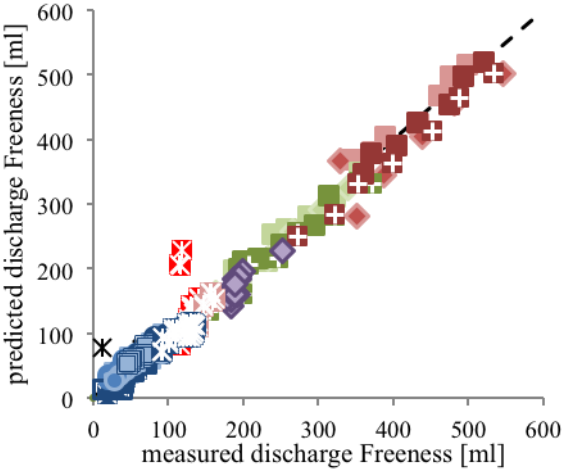

Fig 5. Measured discharge CSF plotted with the predicted discharge CSF from *Eq 6*.

Conclusions

The study has shown using a wide range of refiners from multiple pilot and mill trials that the dimensionless refining power depends on 3 dimensionless variables: a gap parameter, a plate parameter, and a pulp parameter. The dimensionless model is presented in *Eq 1*.

Such a model enables the prediction of refiner gap which has been shown to control fibre and pulp quality for a range of operation and design variables.

Further in *Eq 6*, we demonstrated a similar predictive model for the discharge freeness based on feed freeness, refiner gap and applied net specific energy.

These predictive models provide useful tools for the optimization of the LC refining process, and provide insight into scaling between different diameter refiners.

The dimensionless parameters studied point out an important relationship between the plate gap and the characteristics of the feed pulp. It is recommended that future work done to characterize the refining action include parameters to describe the feed pulp.

Acknowledgements

This work was funded by the Natural Sciences and Engineering Research Council of Canada through the Collaborative Research and Development program, and with the support of our partners BC Hydro, FP Innovations, Catalyst Papers, Howe Sound Pulp and Paper, West Fraser Quesnel River Pulp, Canfor, Andritz, Arkema, Honeywell, WestCan Engineering, Advanced Fiber Technologies, Ontario Power Authority and CEATI international.

A special thanks to Stefan Andersson for his help conducting trials and to Holmen Braviken and Catalyst Paper mills for their help with mill trials.

Literature

Joris, G., (2007): Industrial refining process versus theory, TAPPSA journal, September, http://www.tappsa.co.za/archive3/Journal_papers/Industrial_Refining/industrial_refining.html.

Luukkonen A., Olson J. A. and Martinez D. M. (2010a): Low Consistency refining of mechanical pulp, effect of gap, speed and power, Journal of Pulp and Paper Science, 36(1-2), pp. 28-34.

Luukkonen A., Olson J. A. and Martinez D. M. (2010b): Low Consistency refining of mechanical pulp: A methodology to relate operating conditions to paper properties, Journal of Pulp and Paper Science, 36(3-4) pp 107-111.

Mohlin, U.-B. (2007): Refiner response: gap clearance – power relationship and effect of fibre properties, Refining and Mechanical Pulping, Pira Int., Leatherhead, UK. http://innventia.knowitis.se/upload/14942/Mohlin_RefinerResponse_2007.pdf

Musselman R., Letarte D. and Simard R. (1997): Third stage low consistency refining of TMP for energy savings and quality enhancement, 4th Int. Refining Conf., Fuiggi, Italy, pp 141-147.

Page, D.H. (1989): The beating of chemical pulps - the action and the effect, Transactions of the 9th fundamental research symposium, Cambridge, UK, pp. 1-38.

Manuscript received February 2, 2012
Accepted July 18, 2012

Appendix

Conditions of refiner trials

Sample name	Symbol	Feed CSF ml	BEL km/rev	RPM rev/min	Diameter m (inch)	Motor Size kW	No-load Power kW
Mill A		80	97	509	1.07 (42)	1200	310
Mill B1		140	377	425	1.40 (55)	2000	307
Mill B2		140	486	425	1.47(58)	2000	473
Mill C		245	368	425	1.47(58)	2500	343
Mill D1		150	410	425	1.32 (52)	2000	420
Mill D2		160	320	425	1.47 (58)	2000	660
Mill D3		130	414	320	1.83 (72)	5000	800
Pilot A		116	10.30	1200	0.56 (22)	250	189
Pilot B		115	10.30	1138	0.56 (22)	250	163
Pilot C		108	10.30	800	0.56 (22)	250	61
Pilot D		120	10.30	949	0.56 (22)	250	99
Pilot E		120	14.65	1138	0.56 (22)	250	144
Pilot F		120	14.65	800	0.56 (22)	250	54
Pilot G		115	14.65	1200	0.56 (22)	250	167
Pilot H		120	14.65	800	0.56 (22)	250	54
Pilot I		118	14.65	1200	0.56 (22)	250	167
Pilot J		131	14.65	1200	0.56 (22)	250	167
Pilot C2		387	10.30	1200	0.56 (22)	250	189
Pilot D2		362	10.30	1000	0.56 (22)	250	114
Pilot E2		375	14.65	1200	0.56 (22)	250	167
Pilot F2		383	14.65	1100	0.56 (22)	250	131
Pilot A2		540	10.30	1200	0.56 (22)	250	189
Pilot B2		573	10.30	1000	0.56 (22)	250	114
Pilot G2		549	14.65	1200	0.56 (22)	250	167
Pilot H2		547	14.65	1100	0.56 (22)	250	131